Available online at www.sciencedirect.com
ScienceDirect
Journal of Nuclear Materials 375 (2008) 202–208
journal of nuclear materials
www.elsevier.com/locate/jnucmat

Thermodynamic evaluation of the NaCl–$MgCl_2$–UCl_3–$PuCl_3$ system

O. Beneš *, R.J.M. Konings

European Commission, Joint Research Centre, Institute for Transuranium Elements, P.O. Box 2340, 76125 Karlsruhe, Germany

Abstract

A full thermodynamic description of the quaternary NaCl–$MgCl_2$–UCl_3–$PuCl_3$ system, a Molten Salt Fast Breeder Fuel, is presented. The binary phase diagrams have been assessed in this study and the data were used to extrapolate the higher order systems. To optimize the excess parameters of the liquid phase the modified quasi chemical model has been used, while for the solid solution the classical polynomial model has been applied. From the obtained results a possible fuel composition for the Molten Salt Reactor has been evaluated.

1. Introduction

The Molten Salt Reactor (MSR) is one of the six concepts of the Generation IV nuclear reactors. The major difference compared to the other types of the reactors is the state of the fuel, which is liquid. The reactor system is based on the circulation of the molten salt containing the dissolved fissile material (^{233}U, ^{235}U, ^{239}Pu), circulating from the reactor core to the heat exchanger and back. A big advantage of this system is the possibility to perform the fuel clean-up during operation. It increases the efficiency of the reactor, because most of the fission products that cause the parasitic neutron capturing and slow down the nuclear chain reaction, can be eliminated.

Recently, Mourogov and Bokov [1] proposed the fast breeder molten salt reactor REBUS-3700 based on a U–Pu cycle, where U and Pu are present in the form of trichlorides dissolved in a matrix of liquid NaCl. In general the chlorides have higher vapor pressures and lower thermodynamic stability at high temperatures compared to fluorides, which are generally considered for molten salt reactor applications [2], but on the other hand, they are less aggressive against the structure materials and their melting points are lower. Therefore, more fissile material can be dissolved in the matrix and that is necessary for fast breeder reactor designs. However, the chlorides can only be used in fast reactors and not in thermal reactors, due to the relatively high parasitic neutron-capture cross-section of the chlorine atom.

It is very important to have a thermodynamic description of the fuel, because it is much easier to optimize the fuel choice and to predict its properties. Since the phase diagram of the NaCl–UCl_3–$PuCl_3$ system has not been reported so far the thermodynamic evaluation is performed in this study. Moreover $MgCl_2$ is added to this ternary system in order to see its influence on the melting behavior of the fuel.

2. Thermodynamic modelling

To describe a T–X phase diagram the Gibbs energy equations of all phases and the Gibbs equations of mixing, in case of the presence of solutions, are required. The Gibbs energy function of the pure compounds can be written as in Eq. (1)

$$G(T) = \Delta_f H^0(298\ \mathrm{K}) - S^0(298\ \mathrm{K})T + \int_{298}^{T} C_p(T)\,\mathrm{d}T - T\int_{298}^{T}\left(\frac{C_p(T)}{T}\right)\mathrm{d}T \quad (1)$$

summing the contributions of the enthalpy of formation, the absolute entropy at reference temperature and the heat capacity. There are six condensed compounds considered

* Corresponding author. Tel.: +49 7247 951263; fax: +49 7247 951566.
E-mail address: ondrej.benes@ec.europa.eu (O. Beneš).

0022-3115/$ - see front matter © 2008 Elsevier B.V. All rights reserved.
doi:10.1016/j.jnucmat.2008.01.007

in the studied system. The thermodynamic data of their phases are summarized in Table 1. The data for NaCl were taken from [3] whereas the data for $MgCl_2$ were taken from [4] to remain consistent with the assessment of the NaCl–$MgCl_2$ system presented by Chartrand and Pelton [5]. The data for $PuCl_3$ were obtained from [6] and the data for the solid phase of UCl_3 were taken from [7], whereas the data for the liquid phase of UCl_3 have been estimated by comparison to the data for the early lanthanide trichlorides. The properties of the two intermediate compounds $NaMgCl_3$ and Na_2MgCl_4 have been optimized by Chartrand and Pelton and published in [5].

Since one of the aims of this study was to calculate the vapor pressure of the fuel choice, the following gaseous species have been considered: NaCl, $MgCl_2$, UCl_2, UCl_3, UCl_4, UCl_5, UCl_6, $PuCl_3$ and $PuCl_4$. Thermodynamic data for NaCl and $MgCl_2$ were taken from [4] while the data for all the gaseous species containing actinides are from [8]. Since the vapour pressure is low in the relevant temperature range the gas phase can be treated as ideal mixture.

2.1. Liquid solutions

The modified quasi-chemical model proposed by Pelton and coworkers [9,10] has been used to optimize the excess Gibbs energy functions of the liquid solution. The parameters of this model are the Gibbs energy changes $\Delta g_{AB/Cl}$ for the second nearest neighbor pair-exchange reaction:

$$(A–Cl–A) + (B–Cl–B) = 2(A–Cl–B) \quad \Delta g_{AB/Cl}, \tag{2}$$

where A and B represent the cations and Cl the Cl^- anion. The $\Delta g_{AB/Cl}$ parameter for reaction (2) can be expanded as a polynomial such as

$$\Delta g_{AB/Cl} = \Delta g^0_{AB/Cl} + \sum_{(i+j)\geqq 1} g^{ij}_{AB/Cl} \chi^i_{AB/Cl} \chi^j_{BA/Cl}, \tag{3}$$

where $\Delta g^0_{AB/Cl}$ and $g^{ij}_{AB/Cl}$ are composition independent coefficients (although possibly temperature dependent) obtained from the optimization of the experimental data for binary ACl–BCl solutions. The $\chi_{AB/Cl}$ term is a composition variable and is defined as

$$\chi_{AB/Cl} = \left(\frac{X_{AA}}{X_{AA} + X_{AB} + X_{BB}}\right), \tag{4}$$

where X_{AA}, X_{AB} and X_{BB} represent the cation–cation pair mole fractions. In this model the definition of cation–cation coordination numbers Z^A_{AB}, resp. Z^B_{AB} is required. The values for Na–Na and Mg–Mg unary pairs were taken from [5], while the values for the U–U and Pu–Pu unary pairs were chosen on the basis of the La–La data from previous work [11]. The values for the binary pairs (e.g. Na–Pu pair) were chosen in order to achieve the best reproduction of the phase diagram. For example the definition of the $Z^{Na}_{NaPu} = 1/2 Z^{Pu}_{NaPu}$ defines the maximum short-range ordering near the composition Na_2PuCl_5. It is likely that at this point the excess Gibbs energy function has its minimum and thus the studied system has here the lowest melting point. The cation–cation coordination numbers used in this work are listed in Table 2.

Table 1
$\Delta_f H^0$ (298 K) (kJ mol^{-1}), S^0(298 K) (J K^{-1} mol^{-1}) data and C_p (J K^{-1} mol^{-1}) coefficients for the pure components and intermediate compounds

Compound	$\Delta_f H^0_{(298\ K)}$	$S^0_{(298\ K)}$	a	bT	cT^2	dT^{-2}	Reference
NaCl(g)	−181.420	229.793	37.364	0.00071		−163206.1	[4]
NaCl(l_1)[a]	−394.956	76.076	77.7638	−0.0075312	–	–	[3]
NaCl(l_2)[b]	−390.090	84.506	66.944	–	–	–	[3]
NaCl(s)	−411.120	72.132	45.940	0.016318	–	–	[3]
$MgCl_2$(g)	−392.460	277.027	62.000	0.00014	–	−448180.57	[4]
$MgCl_2$(l_1)[c]	−601.680	129.236	193.4089	−0.3620139	0.00031999	−3788504	[4]
$MgCl_2$(l_2)[d]	−606.887	117.297	92.048	–	–	–	[4]
$MgCl_2$(s)[e]	−641.616	89.629	54.5843	0.0214213	−2.3567E−6	−1112119	[4]
UCl_2(g)	−155.000	339.1	57.807	0.0003464	2.388E−6	158480	[8]
UCl_3(g)	−523.000	380.3	84.018	−0.0034732	3.613E−6	−79890	[8]
UCl_3(l)	−846.433	153.6	150	–	–	–	Estimated
UCl_3(s)	−863.700	163.9	87.78	0.03112	–	458300	[7]
UCl_4(g)	−815.400	409.3	110.634	0.0032375	−3.12E−7	−715600	[8]
UCl_5(g)	−900.000	438.7	128.655	0.01066	−2.661E−6	−710000	[8]
UCl_6(g)	−985.500	438	157.768	9.73E−5	−1.1E−8	−946160	[8]
$PuCl_3$(g)	−647.400	368.62	77.103	0.012997	−4.3125E−6	−188730	[8]
$PuCl_3$(l)	−931.116	170.463	144	–	–	–	[6]
$PuCl_3$(s)	−959.600	161.4	91.412	0.03716	–	−27400	[6]
$PuCl_4$(g)	−792.000	409	110.43	0.0040818	−9.7616E−7	−723430	[8]
$NaMgCl_3$(s)	−1053.136	169.945	90	0.075	–	–	[5]
Na_2MgCl_4(s)	−1463.436	243.996	135	0.1125	–	–	[5]

[a] Temperature range 298–1500 K.
[b] Temperature range 1500–2000 K.
[c] Temperature range 298–660 K.
[d] Temperature range 660–2500 K.
[e] An extra term in the C_p function: $399.177T^{-0.5}$.

Table 2
Cation–cation coordination numbers of the liquid

A	B	Z^{A}_{AB}	Z^{B}_{AB}
Na	Na	6	6
Mg	Mg	6	6
U	U	6	6
Pu	Pu	6	6
Na	Mg	3	6
Na	U	3	6
Na	Pu	3	6
Mg	U	4	3
Mg	Pu	4	6
U	Pu	6	6

The optimized excess Gibbs energy parameters for the binary subsystems are listed below keeping the same notation as proposed by Chartrand and Pelton [12]:

$$\Delta g_{\mathrm{NaMg/ClCl}} = -10395.8 + 660.5\chi_{\mathrm{NaMg}} - 4641.5\chi_{\mathrm{MgNa}} \quad \mathrm{J\,mol^{-1}}, \tag{5}$$

$$\Delta g_{\mathrm{NaU/ClCl}} = -5564.7 - 4602.4\chi_{\mathrm{NaU}} - 3096.2\chi_{\mathrm{UNa}} \quad \mathrm{J\,mol^{-1}}, \tag{6}$$

$$\Delta g_{\mathrm{NaPu/ClCl}} = -8158.8 - 3138\chi_{\mathrm{NaPu}} - 5857.6\chi_{\mathrm{PuNa}} \quad \mathrm{J\,mol^{-1}}, \tag{7}$$

$$\Delta g_{\mathrm{MgU/ClCl}} = 585.8 + 3347.2\chi_{\mathrm{MgU}} + 1882.8\chi_{\mathrm{UMg}} \quad \mathrm{J\,mol^{-1}}, \tag{8}$$

$$\Delta g_{\mathrm{MgPu/ClCl}} = 1966.5 + 418.4\chi_{\mathrm{PuMg}} \quad \mathrm{J\,mol^{-1}}, \tag{9}$$

$$\Delta g_{\mathrm{UPu/ClCl}} = -836.8 - 6276\chi_{\mathrm{PuU}} \quad \mathrm{J\,mol^{-1}}. \tag{10}$$

All the excess Gibbs energy parameters from Eqs. (5)–(10) were obtained in this study. Only the data from Eq. (5) were taken from [5].

2.2. Solid solutions

The only solid solubility that has been reported in the NaCl–$MgCl_2$–UCl_3–$PuCl_3$ system is the continuous solution in the UCl_3–$PuCl_3$ binary. The classical polynomial model has been used to optimize the excess parameters of this solution. The obtained results are

$$\Delta_{xs}G_{\mathrm{(U,Pu)Cl}} = 7000x^2_{\mathrm{UCl_3}}x_{\mathrm{PuCl_3}} \quad \mathrm{J\,mol^{-1}}. \tag{11}$$

2.3. Ternary assessments

The ternary systems have been extrapolated based on the results from the binary assessments applying the Kohler–Toop asymmetric formalism [13]. The end member compounds were divided into two groups of asymmetry. It is most likely that the asymmetric component in the ternary system is the one with a different chemical behavior from the other two. Therefore the first group consists of NaCl and $MgCl_2$ that form ionic liquids compared to UCl_3 and $PuCl_3$ that rather form molecular species in the liquids. Thus in case of a ternary phase diagram that contains two actinide trichlorides the asymmetric component is either the alkali or the alkali earth halide. On the contrary, in case of a ternary that consists of both NaCl and $MgCl_2$ the asymmetric component is the actinide trichloride.

No ternary interaction parameters were introduced in this study.

3. Results

3.1. Binary systems

The NaCl–$MgCl_2$ system has been optimized and described by Chartrand and Pelton [5]. It consists of one eutectic at $T = 732$ K and contains two intermediate phases (Na_2MgCl_4 and $NaMgCl_3$) which decompose peritectically at $T = 748$ K and $T = 739$ K, respectively.

The optimization of the NaCl–UCl_3 system was based on the experimental data by Taube [14]. It is a simple eutectic system with $T = 793$ K and $X_{\mathrm{UCl_3}} = 0.329$. This is in excellent agreement with Taube [14] who derived the same temperature and $X_{\mathrm{UCl_3}} = 0.320$.

NaCl–$PuCl_3$ is another simple eutectic system. Bjorklund et al. [15] have measured this binary and their data were used in our thermodynamic assessment. They reported the eutectic at $T = 726$ K and $X_{\mathrm{PuCl_3}} = 0.360$ whereas we obtained $T = 725$ K and $X_{\mathrm{PuCl_3}} = 0.383$. Thus a very good agreement between our values and the values from [15] was achieved.

The thermodynamic assessment of the $MgCl_2$–UCl_3 system was based on the experimental results by Desyatnik et al. [16]. It is again a simple eutectic system with the experimentally obtained eutectic at $T = 943$ K and $X_{\mathrm{UCl_3}} = 0.35$. Our optimized phase diagram reproduces the same temperature and $X_{\mathrm{UCl_3}} = 0.359$.

$MgCl_2$–$PuCl_3$ is a simple eutectic system that has been experimentally described by Johnson et al. [17]. They reported the eutectic point at $T = 923$ K and $X_{\mathrm{PuCl_3}} = 0.380$. The same values were obtained from our modelling.

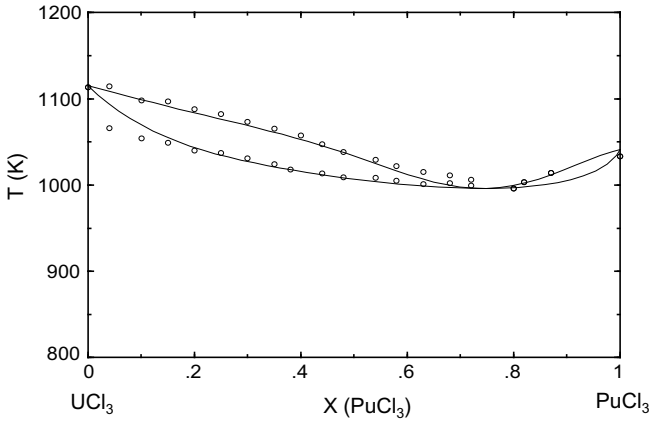

Fig. 1. Calculated phase diagram of the UCl_3–$PuCl_3$ system. ○ results by Morobei et al. [18].

Table 3
Experimental and calculated eutectic equilibria of the $NaCl–UCl_3$, $NaCl–PuCl_3$, $MgCl_2–UCl_3$ and $MgCl_2–PuCl_3$ systems

System A–B	$T_{eutectic}$(exp.) (K)	$X(B)_{eutectic}$ (exp.)	$T_{eutectic}$ (calc.) (K)	$X(B)_{eutectic}$ (calc.)
$NaCl–UCl_3$	793	0.32	793	0.329
$NaCl–PuCl_3$	726	0.36	725	0.383
$MgCl_2–UCl_3$	943	0.35	943	0.359
$MgCl_2–PuCl_3$	923	0.38	923	0.380

$UCl_3–PuCl_3$ system is characterized by the continuous solid solution with the minimum point calculated at $T = 996$ K and $X_{PuCl_3} = 0.746$. This phase diagram has been measured by Morobei et al. [18] reporting the lowest melting point at $T = 996$ K and $X_{PuCl_3} = 0.800$. The calculated phase diagram is shown in Fig. 1 and quite good agreement to the experimental data is evident. Only on the UCl_3 rich side some deviation appears. This disagreement can be suppressed by introducing additional excess Gibbs energy terms, but this would lead to an unrealistic extrapolation.

Because the simple eutectic systems were published earlier and are very well reproduced it is not necessary to show their figures in this work. Only the invariant equilibria calculated in this study and the corresponding experimental results are summarized in Table 3.

3.2. Ternary systems

The $NaCl–MgCl_2–UCl_3$ ternary system is characterized by one quasi-peritectic, two eutectic invariant equilibria and one saddle point (situated between two eutectics). Their corresponding temperatures, composition coordinates and the present solid phases are reported in Table 4, whereas the phase diagram is shown in Fig. 2. To our knowledge this phase diagram has not been described experimentally.

The $NaCl–MgCl_2–PuCl_3$ phase diagram has a very similar shape as the $NaCl–MgCl_2–UCl_3$ diagram. It consists of three invariant points; two quasi-peritectics and one eutectic. The data for the invariant points are summarized in Table 4 and the modelled phase diagram is shown in Fig. 3.

There are no invariant equilibria in the $NaCl–UCl_3–PuCl_3$ system. The melting minimum was found close to the $NaCl–PuCl_3$ binary eutectic, at $T = 722$ K and $X_{NaCl} = 0.594$, $X_{UCl_3} = 0.045$ and $X_{PuCl_3} = 0.360$. No experimental data are known for this system. The calculated phase diagram is plotted in Fig. 4.

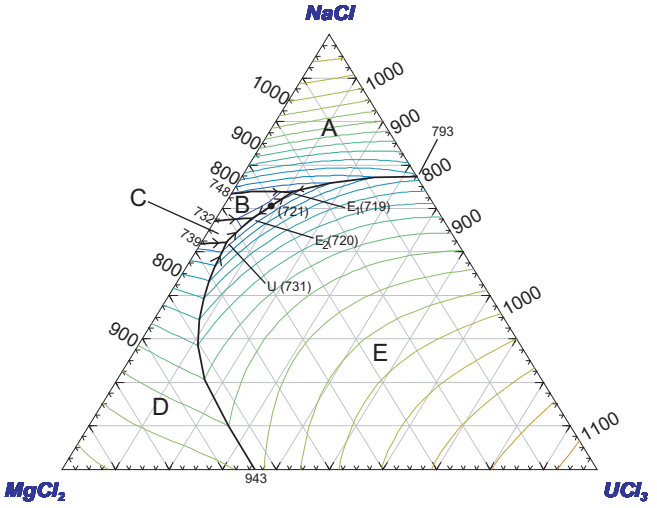

Fig. 2. Calculated liquidus surface of the $NaCl–MgCl_2–UCl_3$ system. Isotherms are labelled in K with interval of 25 K. The dot between E_1 and E_2 corresponds to the saddle point. Primary phase fields: (A) NaCl; (B) Na_2MgCl_4; (C) $NaMgCl_3$; (D) $MgCl_2$; (E) UCl_3.

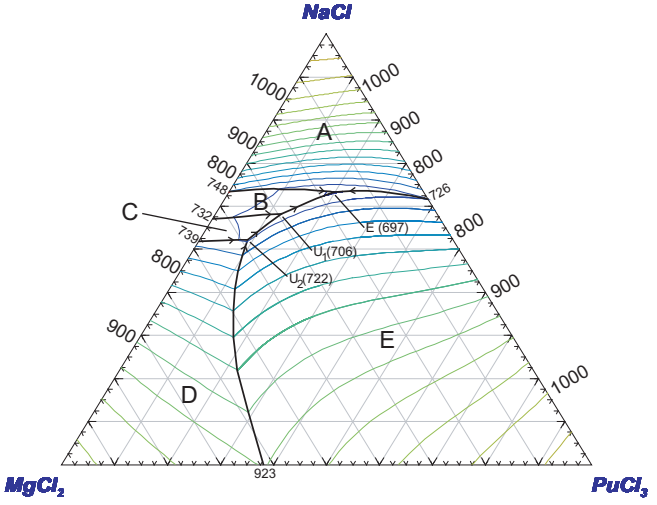

Fig. 3. Calculated liquidus surface of the $NaCl–MgCl_2–PuCl_3$ system. Isotherms are labelled in K with interval of 25 K. Primary phase fields: (A) NaCl; (B) Na_2MgCl_4; (C) $NaMgCl_3$; (D) $MgCl_2$; (E) $PuCl_3$.

Table 4
Calculated invariant points of the ternaries from the $NaCl–MgCl_2–UCl_3–PuCl_3$ system

System (A–B–C)	X_A	X_B	X_C	T (K)	Equilibrium	Solid phases present
$NaCl–MgCl_2–UCl_3$	0.637	0.251	0.112	719	Eutectic	$NaCl + Na_2MgCl_4 + (U,Pu)Cl_3$
	0.578	0.356	0.066	720	Eutectic	$NaMgCl_3 + Na_2MgCl_4 + (U,Pu)Cl_3$
	0.520	0.433	0.047	731	Quasi-peritectic	$MgCl_2 + NaMgCl_3 + (U,Pu)Cl_3$
	0.607	0.089	0.304	721	Saddle point	
$NaCl–MgCl_2–PuCl_3$	0.632	0.171	0.196	697	Eutectic	$NaCl + PuCl_3 + Na_2MgCl_4$
	0.582	0.295	0.124	706	Quasi-peritectic	$Na_2MgCl_4 + NaMgCl_3 + PuCl_3$
	0.521	0.389	0.090	722	Quasi-peritectic	$MgCl_2 + PuCl_3 + NaMgCl_3$
$NaCl–UCl_3–PuCl_3$	0.594	0.045	0.360	722	Minimum	
$MgCl_2–UCl_3–PuCl_3$	0.482	0.148	0.371	913	Minimum	

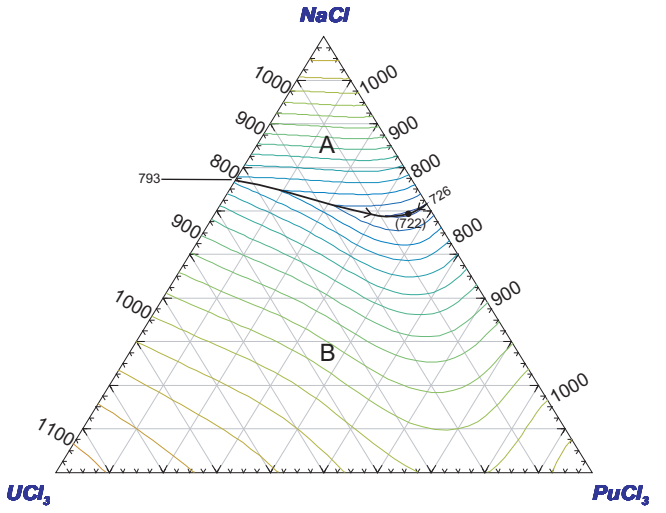

Fig. 4. Calculated liquidus surface of the NaCl–UCl_3–$PuCl_3$ system. Isotherms are labelled in K with interval of 25 K. The dot at the grooves corresponds to the melting minimum. Primary phase fields: (A) NaCl; (B) (U, Pu)Cl_3.

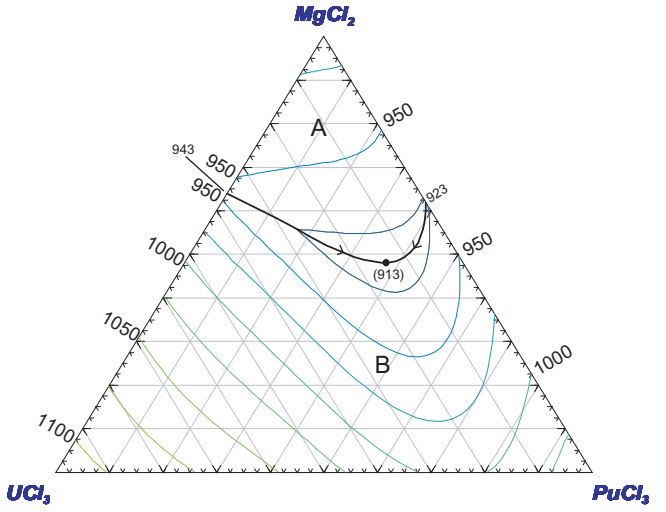

Fig. 5. Calculated liquidus surface of the $MgCl_2$–UCl_3–$PuCl_3$ system. Isotherms are labelled in K with interval of 25 K. The dot at the grooves corresponds to the melting minimum. Primary phase fields: (A) $MgCl_2$; (B) (U, Pu)Cl_3.

The last ternary system to be presented in this study is the $MgCl_2$–UCl_3–$PuCl_3$ system. Similar to NaCl–UCl_3–$PuCl_3$ it is characterized by a melting minimum only, which was calculated at $T = 913$ K and $X_{MgCl_2} = 0.482$, $X_{UCl_3} = 0.148$ and $X_{PuCl_3} = 0.370$. This system has been studied experimentally by Morobei et al. [18] who reported the melting minimum at $T = 908$ K and $X_{MgCl_2} = 0.45$, $X_{UCl_3} = 0.27$ and $X_{PuCl_3} = 0.28$. The experimental temperature is in excellent agreement with our modelled value, but the calculated composition was found to be richer in $PuCl_3$. In order to improve the agreement for the composition we tried to extrapolate this system using the Kohler symmetric approximation, placing $MgCl_2$ in the same group of asymmetry as UCl_3 and $PuCl_3$, but the phase diagram changed very little, shifting the lowest melting point even closer to the $PuCl_3$ side. Another idea would be to use some additional ternary excess Gibbs energy terms, but since the temperature agreement was very good and the details of the results were not reported by Morobei et al. [18], this idea was rejected and the phase diagram was kept as it is shown in Fig. 5.

4. Discussion

As it was stated in the introduction, the main purpose of modelling the NaCl–$MgCl_2$–UCl_3–$PuCl_3$ system was its potential use as a fuel of the Molten Salt Breeder Reactor. In the REBUS-3700 concept [1] NaCl serves as a matrix of the fuel, whereas $PuCl_3$ is the fissile material and $^{238}UCl_3$ is the fertile material. As a breeder design it produces more fissile material than it consumes. The mechanism is based on the neutron capture by ^{238}U resulting in ^{239}Pu. For the REBUS-3700 concept the proposed fresh fuel composition is 55 mol% NaCl, 38 mol% UCl_3 and 7 mol% $PuCl_3$. The concentration of the actinide trichlorides has been chosen in order to sustain the efficient chain reaction on the one hand and to keep the positive breeding ratio on the other hand. Another important fact that influences the fissile material concentration is the total amount of chlorine, which is a neutron absorber, and the strategy of the fuel clean-up. In case of REBUS-3700 it was proposed to have a continuous fuel clean-up with a rate of 35 l/day [1].

In this study the concentrations of $PuCl_3$ (7 mol%) and UCl_3 (38 mol%) [1] have been taken as a composition criterion to be fulfilled when optimizing the fuel choice based on our model. Another criterion to be kept is the melting temperature of the fuel, which should be equal or lower than 873 K. This criterion is also taken from the REBUS-3700 concept [1], where the inlet core temperature was fixed at 923 K applying a safety margin of 50 K.

The NaCl–UCl_3–$PuCl_3$ ternary phase diagram has been modelled in the first approach of our work. As it was described in the previous section, the lowest melting temperature of this system was determined at $T = 721.5$ K, low enough for a nuclear fuel. Nevertheless the composition corresponding to this melting temperature was at $X_{NaCl} = 0.594$, $X_{UCl_3} = 0.045$, $X_{PuCl_3} = 0.360$, for which the concentration of UCl_3 is too low and, on the contrary, the concentration of $PuCl_3$ too high. Since the melting temperature found in our model was very low compared to our criterion ($T = 873$ K) there is sufficient margin for the melting temperature to optimize the composition. Therefore, the isothermal plot at $T = 873$ K for the NaCl–UCl_3–$PuCl_3$ system has been evaluated. It is reported in Fig. 6 where the dotted lines represent the constant concentrations of UCl_3 and $PuCl_3$ at 38 mol% and 7 mol%, respectively. The intersection of these two lines corresponds exactly to the fuel proposal by REBUS-3700 and it can be seen in Fig. 6 that this point lays directly on the border of the liquid surface. Since $T = 873$ K is not the core inlet, but the lower

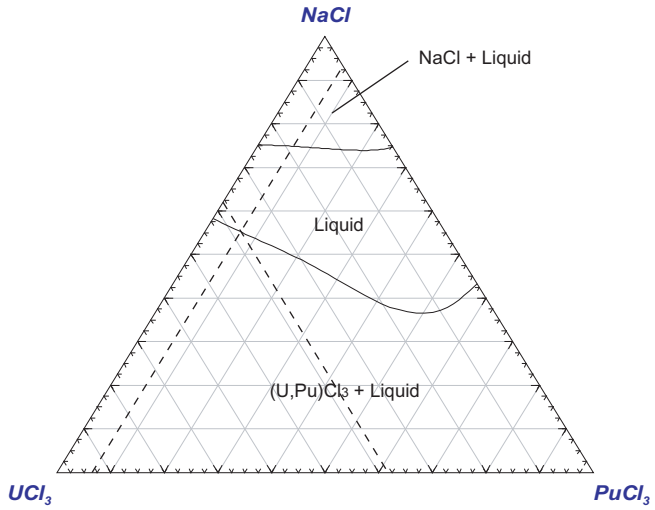

Fig. 6. Isothermal cut of the NaCl–UCl_3–$PuCl_3$ system at $T = 873$ K. Dotted lines represent the constant concentrations of UCl_3 and $PuCl_3$ at 38 mol% and 7 mol%, respectively.

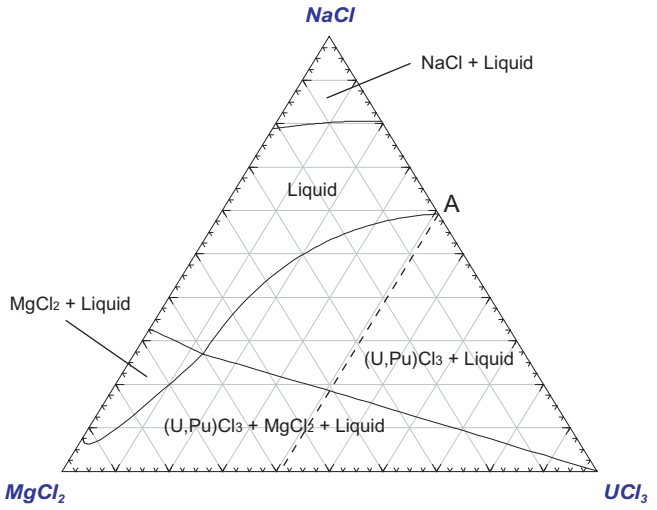

Fig. 7. Isothermal cut of the NaCl–$MgCl_2$–UCl_3 system with constant amount of $PuCl_3$ equal to 7 mol% at $T = 873$ K. Dotted line represents the concentration of UCl_3 equal to 38 mol%.

temperature margin, this composition is acceptable as a fuel for the MSR.

We studied in a further analysis the effect of $MgCl_2$ on the NaCl–UCl_3–$PuCl_3$ system to see its influence on the melting behavior. The main aim of this study was to see if the melting temperature of the fuel decreases with the substitution of NaCl by $MgCl_2$. The same procedure as described in the previous paragraph has been applied. First the lowest melting point, the quaternary eutectic was calculated which was found at $T = 696.5$ K and $X_{NaCl} = 0.629$, $X_{MgCl_2} = 0.165$, $X_{UCl_3} = 0.011$ and $X_{PuCl_3} = 0.195$. The temperature is low enough to fulfill our criteria, but again, as in case of the NaCl–UCl_3–$PuCl_3$ system, the concentration of UCl_3 is very low, while the concentration of $PuCl_3$ is rather high. Next, the pseudoternary phase diagram with a constant amount of $PuCl_3$ of 7 mol% has been calculated for $T = 873$ K. This phase diagram is plotted in Fig. 7, where the dotted line represents the concentration of UCl_3 equal to 38 mol% (in order to fulfill our criteria the fuel composition must be on this line). As it is obvious from the figure this line intersects the liquid field at the NaCl–UCl_3 pseudobinary side (point A in Fig. 7), which means that the concentration of $MgCl_2$ is zero and the composition (point A) corresponds to $X_{NaCl} = 0.550$, $X_{UCl_3} = 0.380$ and $X_{PuCl_3} = 0.070$, the same composition as found in previous paragraph. This observation shows that the addition of $MgCl_2$ to the NaCl–UCl_3–$PuCl_3$ system, where UCl_3 and $PuCl_3$ are kept at 38 mol% and 7 mol%, respectively, increases its melting temperature. Thus it is not a good candidate to be used as a component of the matrix for a fast breeder fuel based on the REBUS-3700 concept.

The vapor pressure of the composition $X_{NaCl} = 0.550$, $X_{UCl_3} = 0.380$, $X_{PuCl_3} = 0.070$ at $T = 1003$ K (the outlet temperature of REBUS-3700 reactor) has been calculated to be $p = 2.25$ Pa, thus very low and acceptable for the MSR assembly.

5. Conclusions

A thermodynamic assessment of the NaCl–$MgCl_2$–UCl_3–$PuCl_3$ system has been made. Our results confirm the fuel proposal ($X_{NaCl} = 0.550$, $X_{UCl_3} = 0.380$, $X_{PuCl_3} = 0.070$) for the Molten Salt Fast Breeder Reactor based on REBUS-3700 concept [1].

Another interesting conclusion is the fact that the addition of $MgCl_2$ does not lower the melting temperature of the fast breeder nuclear fuel that contains 38 mol% of UCl_3 and 7 mol% of $PuCl_3$. Further investigations on the effect of other compounds such as KCl or LiCl on the existing NaCl–UCl_3–$PuCl_3$ system would be of interest for future study.

Acknowledgements

O.B. acknowledges the European Commission for support given in the frame of the program 'Training and Mobility of Researchers'. Dr. Mourogov is thanked for discussion on this topic as well as Petronela Gotcu who collected most of the literature.

References

[1] A. Mourogov, P.M. Bokov, Energ. Convers. Manage. 47 (2006) 2761.
[2] W.R. Grimes, Nucl. Appl. Tech. 8 (1969) 137.
[3] I. Barin, O. Knacke, O. Kubaschewski, Thermochemical Properties of Inorganic Substances, Springer-Verlag, Berlin, 1977.
[4] M.W. Chase Jr. (Ed.), NIST-JANAF Thermochemical Tables Fourth Edition, J. Phys. Chem. Ref. Data, Monograph, 9, 1998.
[5] P. Chartrand, A.D. Pelton, Metall. Trans. A 32 (2001) 1361.
[6] J. Serp, R.J.M. Konings, R. Malmbeck, J. Rebizant, C. Scheppler, J.-P. Glatz, J. Electroanal. Chem. 561 (2003) 143.
[7] R.J.M. Konings, L.R. Morss, J. Fuger, The Chemistry of the Actinide and Transactinide Elements, vol. 4, Springer, Dordrecht, Netherlands, 2006 (Chapter 19).

[8] R. Guillaumont, T. Fanghänel, V. Neck, J. Fuger, D.A. Palmer, I. Grenthe, M.H. Rand, Update on the Chemical Thermodynamics of Uranium, Neptunium, Plutonium, Americium and Technetium, Vol. Chemical Thermodynamics, vol. 5, OECD Nuclear Energy Agency, 2003.
[9] A.D. Pelton, P. Chartrand, G. Eriksson, Metall. Trans. A 32 (2001) 1409.
[10] P. Chartrand, A.D. Pelton, Metall. Trans. A 32 (2001) 1397.
[11] O. Benes, J.P.M. van der Meer, R.J.M. Konings, Comput. Coupl. Phase Diagrams Thermochem. 31 (2007) 209.
[12] P. Chartrand, A.D. Pelton, Metall. Trans. A 32 (2001) 1385.
[13] A.D. Pelton, Calphad 25 (2001) 319.
[14] M. Taube, Fast Reactors Using Molten Chloride Slats as Fuel, Swiss Federal Institute for Reactor Research, Würenlingen, Swiss, 1978.
[15] C.W. Bjorklund, J.G. Reavis, J.A. Leary, K.A. Walsh, J. Phys. Chem. 63 (1959) 1774.
[16] V.N. Desyatnik, Y.A. Izmodenov, Y.T. Mel'nikov, I.F. Nichkov, S.P. Raspopin, Atom. Energ. 26 (1969) 549.
[17] K.W.R. Johnson, M. Kahn, J.A. Leary, J. Phys. Chem. 65 (1961) 1461.
[18] M.P. Morobei, V.N. Desyatnik, O.V. Skiba, N.M. Emel'yanov, Russ. J. Inorg. Chem. 18 (1973) 1628.